INTERNATIONAL JOURNAL FOR NUMERICAL METHODS IN FLUIDS, VOL. 7, 291–303 (1987)

A FINITE ELEMENT METHOD FOR TRANSIENT COMPRESSIBLE FLOW IN PIPELINES

C. BISGAARD, H. H. SØRENSEN* AND S. SPANGENBERG

Oilconsult, Consulting Engineers and Planners A/S, Hovedgaden 2, DK-3460 Birkerød, Denmark

SUMMARY

A finite element method is developed to solve the partial differential equations describing the unsteady flow of gas in pipelines. Excellent agreement is obtained between simulated results and experimental data from a full-scale gas pipeline. The method is used to describe very transient flow (blowout), and to determine the performance of leak detection systems, and proves to be very stable and reliable.

KEY WORDS Gas Flow Pipe Finite Element Transient

INTRODUCTION

Transient flow of gas is an important aspect in the design and operation of pipelines. Gas is a compressible fluid which often exhibits time-varying profiles of flow and pressure in a pipeline. When a steady pattern of flow in a pipeline is disturbed by changing of the flow at either end, a pressure wave is formed which travels away from the source of disturbance. The transient behaviour described above must be properly dealt with if a pipeline system is to be designed and operated effectively.

Transient gas flow in pipelines has been investigated by several authors. Osiadacz[1,2] has used a finite difference method for solving a linear model, in which he neglects the inertia forces. Wiemann[3] has used another method in which, after some simplifications, he solves a set of ordinary differential equations by an Euler method.

In this paper we have used a finite element method combined with an implicit Euler method without making any simplifications of the governing equations.

MATHEMATICAL MODEL

The motion of a continuum is governed by a set of field equations which are common to all continua, and by constitutive equations which identify the intrinsic nature of the continuum.

The law of conservation of mass states that the mass of a volume moving with the gas remains unchanged. It can be written in the form

$$\frac{\partial \hat{\rho}}{\partial t} + \nabla \cdot \hat{\rho} \mathbf{V} = 0, \tag{1}$$

0271–2091/87/030291–13$06.50

Received 24 March 1986
Revised 6 August 1986

often referred to as the Eulerian continuity equation, where $\hat{\rho}$ is the specific density and $\mathbf{V}$ is the velocity.

The principle of conservation of momentum expresses that at any instant the rate of change of momentum of a volume moving with the gas is equal to the sum of surface forces and volume forces acting on the volume. The mathematical formulation of the above principle can be written as

$$\frac{\partial}{\partial t}(\hat{\rho}\mathbf{V}) = -[\nabla\cdot\hat{\rho}\mathbf{V}\mathbf{V}] - \nabla P - \nabla\cdot\tau + \hat{\rho}\mathbf{g}, \tag{2}$$

known as the momentum equation. Where the term $\partial(\hat{\rho}\mathbf{V})/\partial t$ is the rate of increase of momentum per unit volume, $-[\nabla\cdot\hat{\rho}\mathbf{V}\mathbf{V}]$ is the rate of momentum gain by convection per unit volume, $-\nabla P$ is the pressure force per unit volume, $-\nabla\cdot\tau$ is the rate of momentum gain by viscous transfer per unit volume and $\hat{\rho}\mathbf{g}$ is the gravitational force on the element per unit volume.

Equations for compressible gas flow in pipelines

To obtain a mathematical model for one-dimensional gas flow in a rectilinear pipe, it is necessary to reduce the equations (1) and (2) in the following way. The continuity equation becomes

$$\frac{\partial\hat{\rho}}{\partial t} + \hat{\rho}\frac{\partial v}{\partial x} + v\frac{\partial\hat{\rho}}{\partial x} = 0, \tag{3}$$

where the velocity v is the average velocity over the cross-section of the pipeline and $\hat{\rho}$ is the specific density of the gas.

The momentum equation becomes

$$\hat{\rho}\frac{\partial v}{\partial t} + \hat{\rho}v\frac{\partial v}{\partial x} + \frac{\partial P}{\partial x} - \hat{\rho}g\sin\theta + \frac{2f\hat{\rho}v|v|}{D} - \mu\frac{\partial^2 v}{\partial x^2} = 0, \tag{4}$$

where the viscous forces have been approximated by the term

$$\frac{2f\hat{\rho}v|v|}{D} - \mu\frac{\partial^2 v}{\partial x^2}$$

Replacing Newton's law of viscosity by an empirical constitutive equation, which is only valid for flow in pipes. D is the pipe diameter and μ is the dynamic viscosity of the gas.

The friction factor f is calculated by the explicit equation

$$\frac{1}{\sqrt{f}} = -4{\cdot}0\log_{10}\left[0{\cdot}2698(K/D) - \frac{5{\cdot}0452}{Re}\log_{10}\left(0{\cdot}3539(K/D)^{1{\cdot}1098} + \frac{5{\cdot}8506}{Re^{0{\cdot}8981}}\right)\right] \tag{5}$$

proposed by Chen,[4] which is valid over the parameter ranges

$$4000 \leqslant Re \leqslant 4\times10^8,$$

$$5\times10^{-7} \leqslant (K/D) \leqslant 0{\cdot}05.$$

Re is the Reynolds number and K is the roughness of the pipe.

The gravitational force is $\hat{\rho}g\sin\theta$, where g is the acceleration due to gravity and θ is the angle of pipeline inclination with respect to the horizontal plane. The pressure force per unit volume is given by $\partial P/\partial x$, where P is the gas pressure averaged over the cross-section of the pipeline.

By using the chain rule for the term $\partial P/\partial x$ and introducing the molar density ρ, one can rearrange equations (3) and (4) as

$$\frac{\partial \rho}{\partial t} + \rho \frac{\partial v}{\partial x} + v \frac{\partial \rho}{\partial x} = 0 \tag{6}$$

and

$$\rho \frac{\partial v}{\partial t} + \rho v \frac{\partial v}{\partial x} + \frac{1}{M}\left(\frac{\partial P}{\partial \rho}\frac{\partial \rho}{\partial x} + \frac{\partial P}{\partial T}\frac{\partial T}{\partial x}\right) - \rho g \sin\theta + \frac{2f\rho v|v|}{D} - \frac{\mu}{M}\frac{\partial^2 v}{\partial x^2} = 0. \tag{7}$$

Finally, an equation of state is required to complete the description of compressible flow. The ideal gas law states

$$P = Z\rho R T, \tag{8}$$

where Z is the supercompressibility factor, R is the universal gas constant and T is the absolute temperature of the gas. The two derivatives $\partial P/\partial \rho$ and $\partial P/\partial T$, are easily obtained from equation (8), but any equation of state from which it is possible to find the two derivatives $\partial P/\partial \rho$ and $\partial P/\partial T$ could be introduced.

The pipe is regarded as an isolated system without energy exchange with the surroundings. Thus, the law of conservation of energy has not been included in the mathematical model. The gas flow is assumed isothermal, and thus the derivative $\partial T/\partial x$ in equation (7) is equal to zero.

Initial and boundary conditions

The two partial differential equations (6) and (7) form a set of equations which are known as an 'initial value boundary problem'.

To solve the equations in the time domain, it is necessary to define the initial conditions. This is done by solving the stationary problem, in which the derivatives of time are omitted:

$$\rho \frac{\partial v}{\partial x} + v \frac{\partial \rho}{\partial x} = 0 \tag{9}$$

and

$$\rho v \frac{\partial v}{\partial x} + \frac{1}{M}\left[\frac{\partial P}{\partial \rho}\frac{\partial \rho}{\partial x} + \frac{\partial P}{\partial T}\frac{\partial T}{\partial x}\right] - \rho g \sin\theta + \frac{2f\rho v|v|}{D} - \frac{\mu}{M}\frac{\partial^2 v}{\partial x^2} = 0. \tag{10}$$

After solving these equations in the space domain, the initial conditions along the pipe is defined; then the solution in the time domain can be found by integrating the equations (6) and (7), modified by the side boundary conditions.

NUMERICAL METHOD

The basis of the finite element method is the representation of a continuum by an assemblage of sub-divisions called finite elements. The elements are considered interconnected at joints called nodes. The variables in the differential equations are expressed as a linear combination of appropriately selected interpolation functions. Using a weighted residual method the differential equations are transformed into algebraic equations governing each element. These equations are finally assembled to form a global system of algebraic equations for the overall discretized continuum. With proper boundary and initial conditions imposed, solution of these equations will yield the approximate values of the variables at the nodal points.

Interpolation functions

The finite element interpolation functions are characterized by the geometry of the elements, the number of nodes, the choice of specified variables of the nodes and finally the choice of interpolation functions.

A one-dimensional straight line element with two nodes has been chosen to represent flow in pipelines.

Regardless of the geometrical shape, a finite element may be grouped into a Lagrange or a Hermite category. In contrast to the Lagrange family of elements the Hermite category includes derivatives of the variable as well as its values defined at the nodes.

The first derivative of density and the first and second derivatives of velocity are included here, as the gas flow model is also intended as a system for detection of leaks in pipelines (Figure 1). As shown in the next section small leaks are more easily recognized from derivatives of specified variables than from the variables themselves.

The following polynomial expansions have been used as interpolation functions for an approximate determination of velocity and density, respectively:

$$\Phi = a_1 x^5 + b_1 x^4 + c_1 x^3 + d_1 x^2 + e_1 x + f_1, \tag{11}$$

$$\Lambda = a_2 x^3 + b_2 x^2 + c_2 x + d_2. \tag{12}$$

Higher-order polynomials are required since derivatives must be specified at the nodes in addition to the variable itself. Continuity of the variable and the derivatives at the endpoints of the element determines the coefficients.

Finite element formulations of governing equations

A Galerkin finite element method is used to discretize the equations (6) and (7):

$$\int_0^L \left[\frac{\partial \rho}{\partial t} + \rho \frac{\partial v}{\partial x} + v \frac{\partial \rho}{\partial x} \right] \Lambda_\alpha \mathrm{d}x = 0 \tag{13}$$

and

$$\int_0^L \left[\rho \frac{\partial v}{\partial t} + v\rho \frac{\partial v}{\partial x} + \frac{1}{M} \frac{\partial P}{\partial \rho} \frac{\partial \rho}{\partial x} - \rho g \sin\theta + \frac{2f\rho v|v|}{D} - \frac{\mu}{M} \frac{\partial^2 v}{\partial x^2} \right] \Phi_N \mathrm{d}x = 0, \tag{14}$$

where ρ and v are dependent variables and L is the length of the pipe. We choose to use index notation instead of matrix notation and the indices used are defined as $\alpha, \beta = 1, 2, 3, 4$ and $N, M, R = 1, 2, 3, 4, 5, 6$.

The interpolation function for the density, Λ_α, is used as a trial function for the continuity equation, and the interpolation function for the velocity, Φ_N is used as a trial function for the momentum equation, following the discussion on the choice of trial functions given in Reference 5, p. 266.

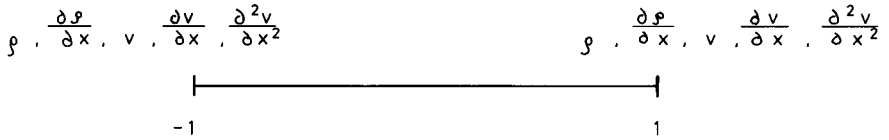

Figure 1. One-dimensional element and the variables specified at the two nodes

The density is approximated by

$$\rho = \sum_{i=1}^{4} \rho_i \Lambda_i \tag{15}$$

and the velocity is approximated by

$$v = \sum_{i=1}^{6} v_i \Phi_i. \tag{16}$$

Equation (13) can be written as

$$A_{\alpha\beta}\frac{\mathrm{d}\rho_\beta}{\mathrm{d}t} + (B_{\alpha\beta M} + C_{\alpha\beta M})\rho_\beta v_M = 0, \tag{17}$$

where

$$A_{\alpha\beta} = \int_0^L \Lambda_\alpha \Lambda_\beta \,\mathrm{d}x,$$

$$B_{\alpha\beta M} = \int_0^L \Lambda_\alpha \Lambda_\beta \frac{\partial \phi_M}{\partial x}\,\mathrm{d}x,$$

$$C_{\alpha\beta M} = \int_0^L \Lambda_\alpha \frac{\partial \Lambda_\beta}{\partial x}\Phi_M \,\mathrm{d}x,$$

and equation (14) can be written as

$$D_{NM\beta}\rho_\beta \frac{\mathrm{d}v_M}{\mathrm{d}t} + E_{NMR\beta} v_M v_R \rho_\beta + \frac{1}{M} F_{N\beta}\left(\left[\frac{\partial P}{\partial \rho}\right]\right)$$

$$- H_{N\beta}\sin\theta\rho_\beta + \frac{2f}{D} Q_{NMR\beta} v_R |v_M| \rho_\beta - \frac{\mu}{M} R_{NM} v_M = 0, \tag{18}$$

where

$$D_{NM\beta} = \int_0^L \Phi_N \Phi_M \Lambda_\beta \,\mathrm{d}x,$$

$$E_{NMR\beta} = \int_0^L \Phi_N \Phi_M \frac{\partial \phi_R}{\partial x}\Lambda_\beta \,\mathrm{d}x,$$

$$F_{N\beta}\left(\left[\frac{\partial P}{\partial \rho}\right]\right) = \int_0^L \left[\frac{\partial P}{\partial \rho}\right]\Phi_N \frac{\partial \Lambda_\beta}{\delta x}\,\mathrm{d}x,$$

$$H_{N\beta} = \int_0^L \Phi_N \Lambda_\beta \,\mathrm{d}x,$$

$$Q_{NMR\beta} = \int_0^L \Phi_N \Phi_M \Phi_R \Lambda_\beta \,\mathrm{d}x,$$

$$R_{NM} = \int_0^L \Phi_N \frac{\partial^2 \phi_M}{\partial x^2}\,\mathrm{d}x.$$

The integrals, except $F_{N\beta}([\partial P/\partial\rho])$, are independent of time and space when the element geometry is defined, and they can be calculated at the start of the computer calculation and used throughout the whole calculation. It is necessary to calculate $F_{N\beta}([\partial P/\partial\rho])$ for each element at all time steps, since $\partial P/\partial\rho$ is a function of both time and space. Gauss quadrature is used for the integration where

the order of the Gauss quadrature is adjusted to the order of the polynomial following the rules given in Reference 5, p. 202.

First, a third-order Runge–Kutta method was used for the time integration:

$$y^{i+1} - y^i = \frac{\Delta t}{6}(K_1 + 4K_2 + K_3),$$

$$K_1 = f(x^i, y^i),$$

$$K_2 = f(x^i + \tfrac{1}{2}\Delta t, y^i + \tfrac{1}{2}\Delta t K_1),$$

$$K_3 = f(x^i + \Delta t, y^i - \Delta t K_1 + 2\Delta t K_2),$$

but this method was not stable for the time integration. It was impossible to maintain a steady-state situation. The reason for the instability was not discovered. A possible explanation could be that the Runge–Kutta method is not stable because the differential equations are non-linear. A fully implicit Euler integration method was tried instead:

$$y^{i+1} - y^i = \Delta t f^{i+1}. \tag{19}$$

This method was used without any stability problems. The resulting non-linear system was solved by the Newton–Raphson method.

In each iteration it is necessary to solve a set of linear equations. The matrix is sparse with a bandwidth of ten. A standard subroutine for profile equation-solving, called UACTCL,[6] was used for solution of the linear equations.

SIMULATION OF TRANSIENT GAS FLOW IN PIPELINES

Comparison of full-scale measurements and calculation

A comparison of full-scale measurements and corresponding finite element calculations has been made. The results are given below.

Full-scale measurements were carried out in 1979 on a 77·33 km gas pipeline from Neustadt through Sörzen to Unterföhring in Germany (Figure 2). The measurements are described in Reference 7. Pressure, temperature and flow were measured in Neustadt and Unterföhring, while pressure and temperature were recorded in Sörzen. The measurements were taken simultaneously every fifth minute from 9.00 a.m. to 2.30 p.m. during very transient flow conditions.

The pipeline was closed at Unterföhring at 9.00 a.m. while the volume flow at Neustadt was kept constant. At 11.00 a.m. the pressure at Neustadt had increased from 7·2 bar to 9·5 bar, close to the maximum permissible pressure. The pipeline was opened again at Unterföhring and the pressure decreased, until normal flow conditions were re-established.

The thermodynamic data and the dynamic viscosity of the gas are given in Table I.

The pressure and the volume flow measured at Neustadt and Unterföhring, respectively, have been used as boundary conditions for the simulation (Figures 3 and 4).

Before the transient calculation was carried out, the roughness of the pipe wall was adjusted, until the measured and calculated parameters for stationary flow were identical. The roughness for the pipe sections Neustadt–Sörzen and Sörzen–Unterföhring thus became 0·3 mm and 0·05 mm.

The finite element model consisted of 21 elements, and the calculations were carried out with a time step length of 300 s.

The measured and the calculated pressure variations at Sörzen and Unterföhring are compared in Figure 5. Results for every 15 min have been plotted. The mean and the maximum discrepancy

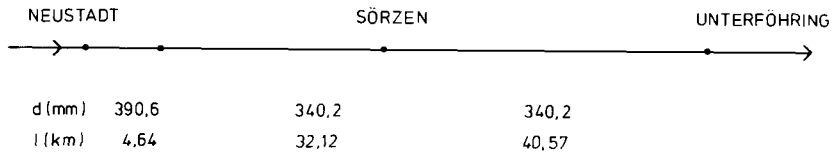

Figure 2. Pipeline from Neustadt through Sörzen to Unterföhring with specification of inner diameter and pipe length

Table I. Thermodynamic data and the dynamic viscosity of the gas

Temperature	(K)	286
Compressibility factor		0·98
Molar weight	(kg/mole)	$1{\cdot}65 \times 10^{-2}$
Dynamic viscosity	(Pa s)	$9{\cdot}84 \times 10^{-6}$

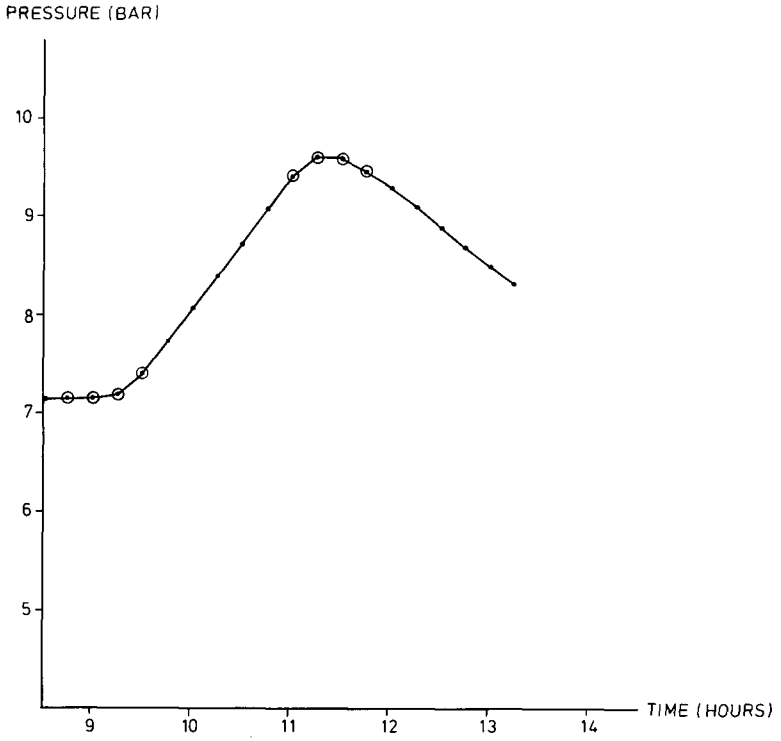

Figure 3. Pressure boundary conditions at Neustadt

between the measured and calculated pressure values are 0·04 bar and 0·09 bar, respectively, and the error of the pressure measurements is smaller than 0·04 bar.[7]

Leak detection

Pipeline simulation models can be used to identify leakages. The predictions from the simulator are compared with measurements from the pipeline. If there is discrepancy between the measured

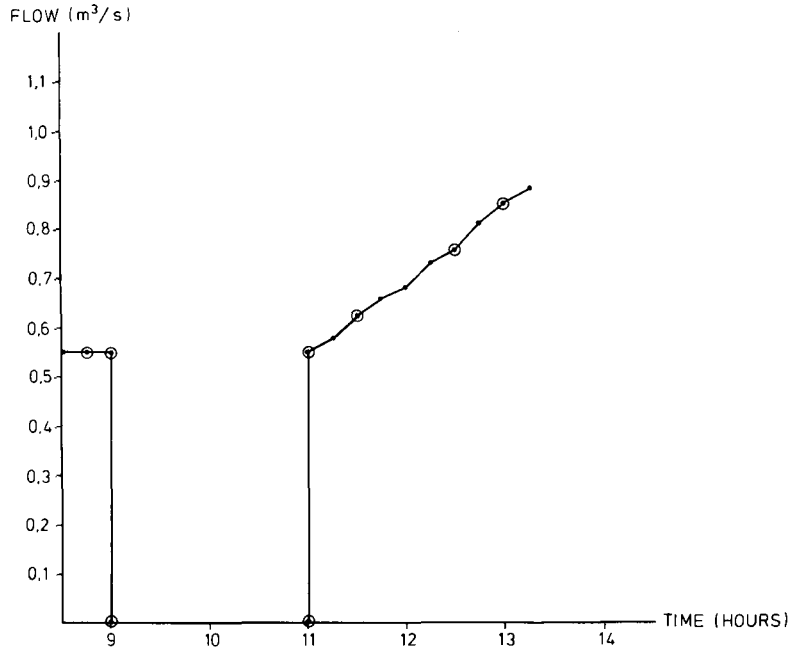

Figure 4. Volume flow boundary conditions at Unterföhring

and predicted values, a leak may exist if the discrepancy is above a certain threshold value. The threshold value is determined by the error of measurements and the error of prediction, and is normally for a practical implementation determined by experiments in which an artificial leak is created.

A leakage in the pipeline from Neustadt to Unterföhring has been simulated (Figure 6) in order to determine the performance of a leak detection system for a low pressure pipeline.

The normal steady flow conditions (Table II) were changed by decreasing the pressure by 0·02 bar at a position 4·76 km from Sörzen. The pressure drop corresponds to a sudden decrease in the mass flow of approximately 12 per cent. The volume flow at Unterföhring was kept constant during the simulation.

The effect of the sudden change of the steady state is given in Table III. Velocity and pressure variations have been calculated for a position along the pipeline corresponding to Sörzen. The variations are given as percentages of the steady-state values.

It appears that the velocity and pressure gradients were much more sensitive to the change of state than the main variables. The maximum decreases in velocity and pressure were approximately 3 per cent and 0·3 per cent, respectively, at a position 4760 m from the leakage.

The results give an indication of the necessary accuracy of the flow and pressure measurements.

Simulation of outflow from a rupture

In this example the results of a simulation of outflow from a rupture on a horizontal high pressure pipeline are described. The outflow of gas into the atmosphere has been calculated until a new steady-state condition occurs.

The pipeline is in contact with a gas reservoir at one end. The rupture occurs 2048 m from the reservoir (Figure 7). The fluid is assumed to behave like an ideal gas with constant specific heat

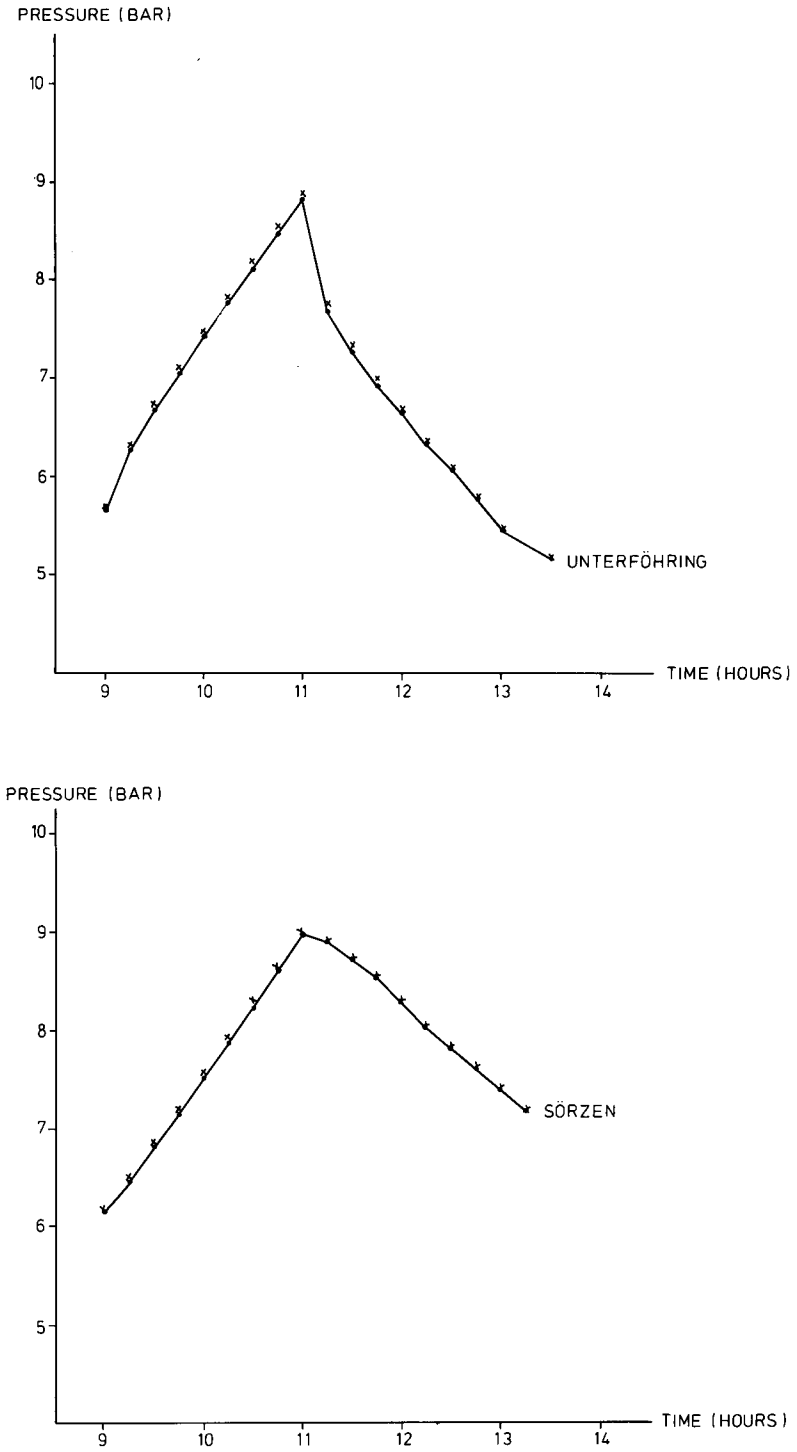

Figure 5. Comparison of measured and calculated pressure variations at Unterföhring and Sörzen. Calculated data are indicated by (×) and the experimental data are indicated by straight lines

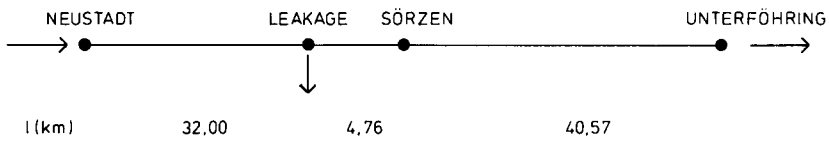

Figure 6. The effect of a leakage in a low pressure pipeline has been determined

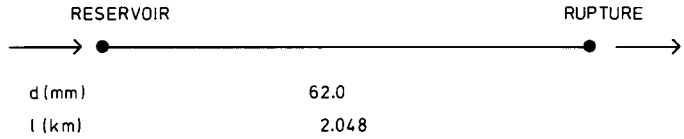

Figure 7. High pressure pipeline from the reservoir to the rupture with specification of inner diameter and length

Table II. Steady-state conditions at Sörzen before leakage: v is velocity, M is massflow and P is pressure

v_s	$\left(\frac{\partial v}{\partial x}\right)_s$	M_s	P_s	$\left(\frac{\partial P}{\partial x}\right)_s$
(m/s)	(1/s)	(kg/s)	(bar)	(bar/m)
5·034	$1{\cdot}914 \times 10^{-5}$	2·007	6·186	$-1{\cdot}667 \times 10^{-5}$

Table III. Velocity and pressure variations at Sörzen after leakage. The variations are given as percentages of the steady-state values

Time after leakage (s)	$\frac{v}{v_s}$ (%)	$\frac{(\partial v/\partial x)}{(\partial v/\partial x)_s}$ (%)	$\frac{M}{M_s}$ (%)	$\frac{P}{P_s}$ (%)	$\frac{(\partial P/\partial x)}{(\partial P/\partial x)_s}$ (%)
10	98·654	273·0	98·623	99·968	96·2
20	99·157	354·4	97·082	99·922	93·2
30	96·482	305·1	96·371	99·885	92·7
40	96·466	231·1	96·332	99·861	93·2
50	96·497	181·7	96·547	99·846	93·9
60	96·954	153·2	96·793	99·835	94·4
120	97·861	114·3	97·668	99·802	95·9
180	98·281	106·0	98·073	99·788	96·6
240	98·536	102·9	98·318	99·779	97·1
300	98·712	101·3	98·488	99·773	97·4

Table IV. Thermodynamic data and the dynamic viscosity of the gas

Temperature	(K)	286
Compressibility factor		0·75
Molar weight	(kg/mole)	$1{\cdot}82 \times 10^{-2}$
Dynamic viscosity	(Pa s)	$2{\cdot}2 \times 10^{-5}$

flowing through a convergent nozzle. Thus the magnitude of the velocity of the gas at the exit is equal to the local speed of sound as long as the pressure at the exit, P_t, exceeds the pressure of the surroundings, P_B, as given in the following equation from Reference 8:

$$P_t > \left[\frac{2}{\gamma+1}\right]^{-\gamma/(\gamma-1)} P_B. \tag{20}$$

With the specific heat ratio, γ, equal to 1·28, equation (20) becomes $P_t > 1{\cdot}82 P_B$.

During normal steady-state conditions the pressure at the inlet of the pipe is 80 bar and the velocity of the gas at a position corresponding to the rupture is 5·8 m/s.

In the calculations it is assumed that the outflow velocity has attained the local velocity of sound one second after the rupture has occurred. As the pressure of the exit is greater than 1·82 times the atmospheric pressure, the outflow velocity is kept equal to the velocity of sound during the rest of the simulation.

The thermodynamic data and the dynamic viscosity of the gas are given in Table IV.

The calculations have been carried out with 21 elements and a time step length of 0·5 s.

The outflow at the rupture is depicted in Figure 8 from the moment the rupture occurs to when a new steady-state condition appears.

CONCLUSIONS

A finite element method for the simulation of gas flow in pipelines has been formulated. The method is an alternative to existing finite difference methods.

Results from the computer program have successfully been compared with actual process data from a full-scale pipeline.

The method has been used to determine the performance of leak detection systems for natural gas pipelines.

ACKNOWLEDGEMENTS

The authors gratefully acknowledge the financial assistance provided by the Danish Ministry of Industry. The authors wish to thank J. A. Hansen for useful discussions concerning thermodynamics, and Dr. Ole Hassager for help with the numerical methods.

NOTATIONS

D Diameter of the pipe
f Friction factor
g Acceleration due to gravity
M Molar weight
P Static pressure or negative component of the stress normal to the surface

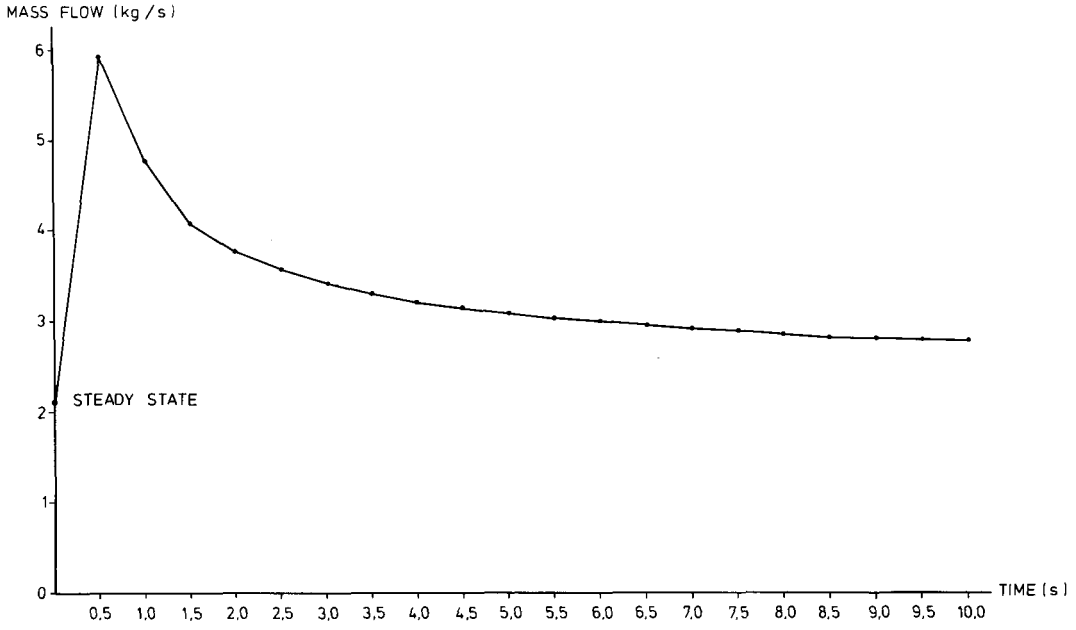

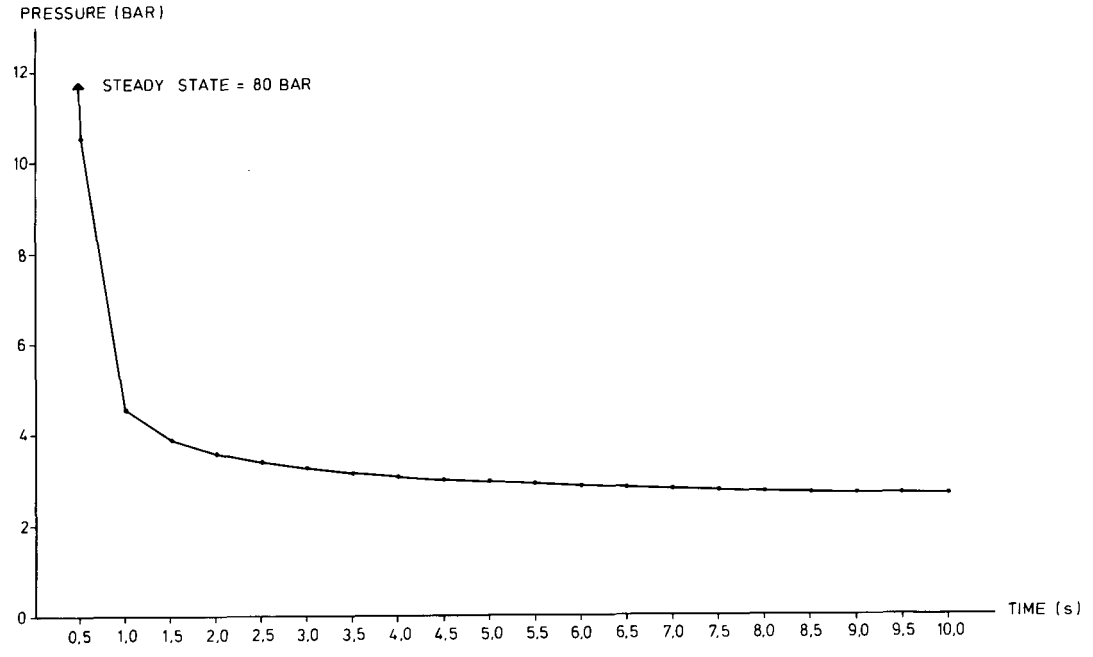

Figure 8. Simulation of outflow from a rupture in a high pressure gas pipeline. The pressure at the position of the rupture is depicted in the lower diagram. During the whole simulation the outlow pressure is greater than 1·82 times the pressure of the surroundings. The flow is thus sonic at the rupture

R	Gas constant
Re	Reynolds number
t	Time
$\mathbf{V}$	Velocity, a vector point function
v	Average velocity of the gas
x	Distance co-ordinate
θ	Angle of pipeline inclination with respect to the horizontal plane
μ	Dynamic viscosity
ρ	Molar density of the gas
$\hat{\rho}$	Specific density of the gas
$\boldsymbol{\tau}$	Viscous stress tensor
∇	Divergence operator

REFERENCES

1. A. Osiadacz, 'Optimal numerical method for simulating flow of gas in pipelines', *Int. j. numer. methods fluids*, **3**, 125–135 (1983).
2. A. Osiadacz, 'Simulation of transient gas flows in networks', *Int. j. numer. methods fluids*, **4**, 13–24 (1984).
3. A. Weimann, *Programsystem GANESI, Dokumentationsbericht III*, Gesellschaft für Kernforschung MBH Karlsruhe, 1977.
4. N. H. Chen, 'An explicit equation for friction factor in pipe', *Ind. Eng. Chem. Fund*, **18**, 296 (1979)
5. T. J. Chung, *Finite Element Analysis in Fluid Mechanics*, McGraw-Hill, 1978.
6. O. C. Zienkiewicz, *The Finite Element Method*, Third edn, McGraw-Hill, 1977.
7. K. Eibl and A. Weimann, *Experimentelle Validierung des Programsystems GANESI*, Gesellschaft für Kernforschung MBH, Karlsruhe, 1977.
8. J. A. Owczarek, *Fundamentals of Gas dynamics*, International Textbook Company, Pennsylvania, 1968.